

# On Tracking the Dynamics of the Gut's Butyrate Factories

Sandhya Vasudevan, BT24D401

**Abstract:** This project investigates the dynamics of the cross-feeding gut microbe pair — *Faecalibacterium prausnitzii* and *Bifidobacterium adolescentis* which together drive efficient butyrate production. Butyrate is renowned to be a vital metabolite that performs several regulatory roles in the human body, mainly the alleviation of neurological conditions. In terms of dynamics, this work tracks the species' growth and butyrate secretion profiles across different nutritional conditions. An ecological perspective is also provided in terms of characterising their interaction profile and testing the Black Queen Hypothesis. Further, dynamic flux balance analysis is employed to explore growth patterns and butyrate efflux over time. Finally, *Lactobacillus brevis* is added as a third member, and the effects are noted. Another ecological viewpoint is to sequentially add the three species to gauge which combination of succession could be ecologically feasible for the community to thrive. The genome-scale metabolic models of the species were employed for the simulations. Results ascertain that the gluten-free and high-fibre diets support maximum butyrate production with *Bifidobacterium adolescentis* behaving like a parasite in most diets. When grown in monoculture and co-culture, *F. prausnitzii* and *B. adolescentis* declined in growth, with butyrate production being higher in co-culture compared to monoculture. Sequential invasion of these two species along with *L. brevis* revealed that certain orders of invasions support both growth and butyrate production. In sum, the study paves the way for the optimal design of probiotic intervention strategies to get the best outcomes.

**Keywords:** Butyrate, Cross-Feeding, Gut Microbes, Probiotics, Genome-Scale Metabolic Models

## 1. INTRODUCTION

Butyrate is a crucial metabolite for our body, ranging from maintaining the homeostasis of the colonocytes in the gut to keeping a check on the immune system's inflammatory responses and preventing certain cancers (e.g., colon cancer). This short-chain fatty acid is produced by microbes in our gut via the fermentation of dietary fibres. It is a key player in the crosstalk between the gut and the brain (the gut-brain axis), exerting neuroprotective effects by crossing the blood-brain barrier. In the human gut, butyrate is generally observed to be produced by cross-feeding microbes where one organism is a butyrate producer and the other(s) supply sufficient amounts of precursors such as acetate or lactate that can boost butyrate production in the former (Singh et al. (2023)).

One such classic combination is the duo: *Faecalibacterium prausnitzii* (butyrate producer) and *Bifidobacterium adolescentis* (acetate producer). Studies have reported that the former cross-feeds on acetate secreted by the latter to produce enhanced butyrate in the co-culture as against the monoculture. (Rios-Covian et al. (2015), Rivi re et al. (2016)) *B. adolescentis* is already being used as a probiotic, primarily because of its role in producing the neurotransmitter GABA, to deal with psychological disorders. (Duranti et al. (2020), Shao et al. (2024), Hazan et al. (2022)). *F. prausnitzii*, regarded as the sentinel of the gut, is being considered a potential Next-Generation probiotic in recent times. (He et al. (2021)) If both organisms are administered as probiotics, it can help alleviate neurological disorders (or any inflammation, too) in a two-way strategy, via

GABA and butyrate. Since the human gut is home to several hundred species of microbes, and each gut has a unique microbiome, it is not easy to simulate the growth of the bacteria under consideration along with all the gut microbes. So, with only this pair under consideration, *Lactobacillus brevis*, another probiotic, was eventually added, to study the effects. With the motivation set, the following are the objectives of this undertaking.

### 1.1 Objectives

- (1) To find the diet which best supports butyrate production by *F. prausnitzii* (in the community set-up). In case of any variations, to try understanding the metabolic flux picture in each case.
- (2) To identify the nature of the ecological interaction between the two species.
- (3) To test the Black Queen Hypothesis (BQH) and how susceptible the species are to gene deletions. This evolutionary question arises since *F. prausnitzii* receives acetate from its counterpart. Can it afford to lose one or more of its intrinsic acetate-producing genes?
- (4) To simulate growth dynamically and understand growth and butyrate efflux patterns. When is butyrate produced effectively?
- (5) To introduce a new member (a probiotic invader) and study how the dynamics change, and perform sequential invasion to study ecological consequences.

When we get insights into these interaction dynamics, we will be better equipped to design suitable probiotic intervention strategies.

## 2. METHODS

### 2.1 Models and Tools Employed

- (1) **Models:** The genome-scale metabolic models of *Bifidobacterium adolescentis*\_ATCC 15703, *Faecalibacterium prausnitzii*\_ERR1022279 and *Lactobacillus brevis*\_DSM\_20054 were downloaded from the AGORA 2 database.
- (2) **Diets:** 11 diet files were downloaded from the VMH database and modified to AGORA diets using a function made available in an earlier paper (Singh et al. (2022)). In addition to these 11 diets, two commonly used AGORA diets were also employed (Magnúsdóttir et al. (2017)). The composition of the diets can be found at the Virtual Metabolic Human’s website: VMH
- (3) **Simulations:** These were carried out using MATLAB (2024b), COBRA Toolbox (v3) (Heirendt et al. (2019)) for flux balance analysis (FBA), and COMETS (Dukovski et al. (2021)) for dynamic FBA simulations. COMETS was implemented in a conda environment using Python 3.9.21.

All codes and the YAML file of the conda environment can be accessed at the GitHub repository: [Link to repository](#)

### 2.2 Evaluation of the models’ qualities

Several models for the three organisms were downloaded from the AGORA 2 database, and their qualities were tested using MEMOTE. The models for *B.adolescentis* (ATCC 15703) *F. prausnitzii* (ERR1022279) and *L.brevis* (DSM 20054) had MEMOTE scores of 89%, 85% and 85% respectively. These scores ranked the highest among the models considered and were taken forward for the study.

### 2.3 Comparison of growth and butyrate production across diets — monoculture vs co-culture

As a first step, the models of *B.adolescentis* and *F. prausnitzii* were loaded into MATLAB and monoculture FBA simulations were performed across the 13 different diets. Next, a community comprising both species was formed, and co-culture simulations were carried out in all the diets. The simulations were performed mimicking an anaerobic environment as oxygen is believed to be scarce in the human gut (this was done by setting the lower bounds of the oxygen reactions to zero). The objective function for all FBA simulations was set to maximise biomass (in the case of the community, the community’s overall biomass). For every simulation, flux variability analysis (FVA) was carried out for the butyrate exchange reaction of *F. prausnitzii* to gauge the maximal capacity for butyrate production.

The growth of both organisms (in terms of biomass) was recorded across diets in monoculture and co-culture. The maximal butyrate production from the FVA was also recorded for all diets in the monoculture and co-culture by *F. prausnitzii*.

In addition, to verify cross-feeding of acetate, in the community, the acetate exchange fluxes were also tracked across all 13 diets.

### 2.4 Characterising the interaction types across diets

The interaction type of the two organisms in co-culture was characterised based on the following formula for all the diets (Sambamoorthy and Raman (2022)).

$$\alpha_1 = \frac{v_{1,\text{com}} - v_{1,\text{ind}}}{v_{1,\text{ind}}} \times 100$$

$$\alpha_2 = \frac{v_{2,\text{com}} - v_{2,\text{ind}}}{v_{2,\text{ind}}} \times 100 \quad (1)$$

### 2.5 Testing the Black Queen Hypothesis

Another intriguing question was, since *B.adolescentis* secretes an excess of acetate, can *F. prausnitzii* afford to lose one or more of its internal acetate-producing genes as both organisms evolve to conserve energy (typical case of the Black Queen Hypothesis). Acetate-producing genes in *F. prausnitzii* include ACKr, PTAr, etc. These genes were knocked out individually and in several combinations using the gene deletion function in MATLAB.

### 2.6 Flux Distribution Analysis

This was performed on the butyrate and internal acetate synthesis pathways in *F. prausnitzii* as well as the internal acetate synthesis pathways in *B.adolescentis*. These were done by starting at the final butyrate and acetate reactions and working our way backwards and going upto reactions in glycolysis, thereby linking the availability of C-sources with butyrate/acetate production.

### 2.7 Dynamic FBA simulations

#### Growing the species pair as a co-culture

Computation Of Microbial Ecosystems in Time and Space (COMETS) was employed to carry out dFBA simulations. The tool gives us control in fixing the space available for the microbes to grow, initial concentrations of both microbes, the duration of the simulations, along with an option of batch or chemostat set-up. Dukovski et al. (2021) In this project, simulations were carried out in a chemostat set-up with a dilution rate of  $0.017 \text{ h}^{-1}$  (average colon transit time is around 60h). Values of  $K_m$  and  $V_{max}$  were set to the average of *E.coli* cells as reported in the COMETS publication. The high-fibre diet was used for all simulations, whose durations lie between 60 and 100h.

#### Sequential Invasion

This is an approach to dynamically add one species after the other by giving a time gap between consecutive additions. It helps in understanding how the presence of one or more species in an environment steers the growth (or otherwise) of another species that is newly added. It also hints at possible evolutionary trajectories. Sequential Invasion was simulated by running COMETS for the first member (the pioneer) for a certain duration of time. The coordinates of the last time-point set the stage for the subsequent species (the invaders), which were also simulated in a similar fashion. In this project, up to three-step invasions were performed.

### 3. RESULTS AND DISCUSSION

#### 3.1 Comparison of growth and butyrate production across diets — monoculture vs co-culture

From fig. 1, which compares growth (in terms of biomass flux) of each species in monoculture and co-culture, we can infer that *F. prausnitzii*'s growth declines in co-culture in the majority of the diets. In contrast, *B. adolescentis* grew exceedingly better in co-culture as compared to monoculture (where its growth was very less compared to *B. adolescentis*'s monoculture growth) in most dietary conditions, as evident from fig. 2. Interestingly, an inverse correlation was observed: in all diets where one species performed better in co-culture, the other species declined with respect to the monoculture growth.

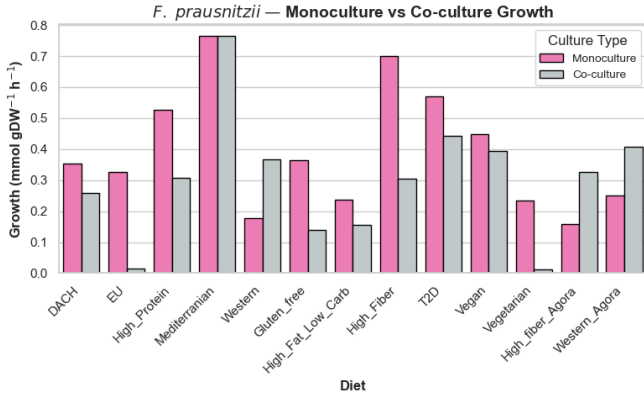


Fig. 1. Growth of *F. prausnitzii*: Monoculture vs Co-culture

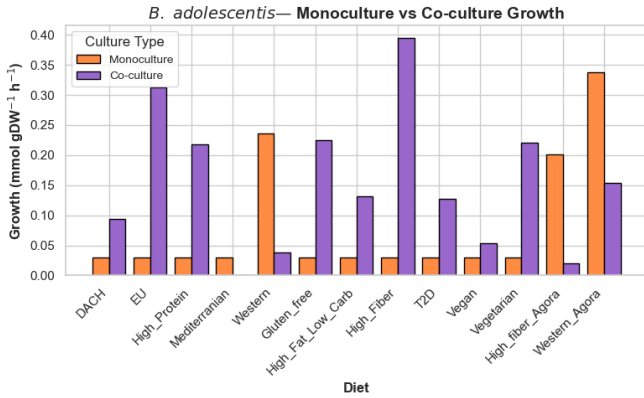


Fig. 2. Growth of *B. adolescentis*: Monoculture vs Co-culture

In co-culture, despite *F. prausnitzii*'s reduction in growth compared to monoculture, it outbeats the abundance of *B. adolescentis* in more than half of the dietary conditions (fig. 3). This is not a surprise since the monoculture growth *F. prausnitzii* is much higher than *B. adolescentis*. Owing to this, even after reduction, the growth is higher than its counterpart in the community setting.

Fig. 4 illustrates the maximal capacity of butyrate production (in terms of fluxes) from FVA performed on the community. The monoculture FVA of *F. prausnitzii* serves

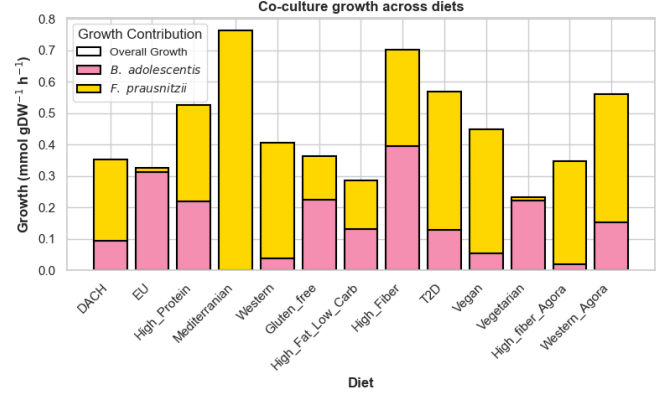


Fig. 3. Growth distributions of both organisms in co-culture

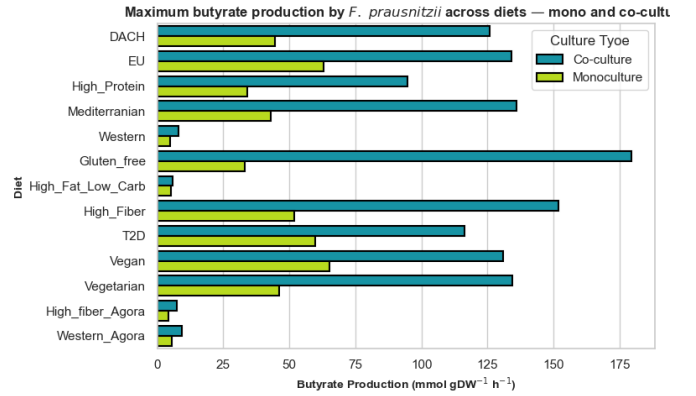


Fig. 4. Butyrate production by *F. prausnitzii*: Monoculture vs Co-culture

as a baseline for comparing the fluxes in co-culture. There are two main observations: one, across all 13 diets, the butyrate flux in co-culture exceeds that in monoculture (upto 3.5 fold). This phenomenon has already been reported earlier and is attributed to *F. prausnitzii* consuming the acetate released by *B. adolescentis*. The second observation is that the gluten-free diet followed by the high-fibre diet rank as the top two diets that support extremely high butyrate fluxes. In these two diets, the abundances of both species are also well-distributed. This suggests that if these organisms are administered as probiotics (or are already abundant in the gut, which is normally the case), then, following either of these two diets will boost butyrate production. Next, to confirm cross-feeding of acetate between the two species in co-culture, the acetate fluxes were tracked and plotted. A clear correspondence between the acetate released by *B. adolescentis* and consumed by *F. prausnitzii* was noticed in 10 diets (fig 5).

#### 3.2 Characterising the Interaction Types Across Diets

The interaction type of the two organisms was characterised based on equation (1) for all the diets (Table 1, the column 'Interaction Type' includes the initial of the species benefiting from the interaction). It was found to be mostly parasitic with *B. adolescentis* gaining advantage from *F. prausnitzii* (but for the Mediterranean diet where

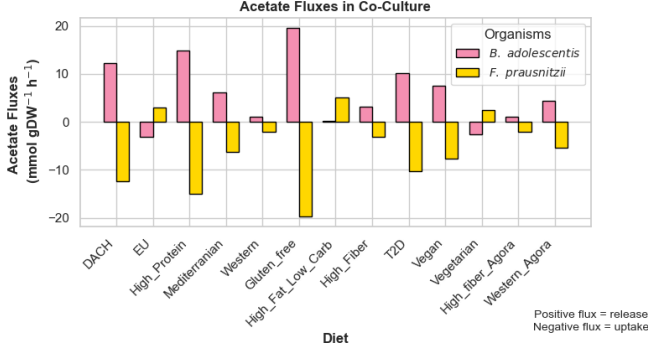


Fig. 5. Acetate fluxes in *F. prausnitzii*

Table 1. Interaction types between *B.adolescentis* and *F. prausnitzii* across diets

Diet	$\alpha(B.adolescentis)$	$\alpha(F.prausnitzii)$	Interaction Type
DACH	216.521691	-26.600442	Parasitism (B.a)
EU	953.402064	-95.667112	Parasitism (B.a)
High_Protein	635.94123	-41.507612	Parasitism (B.a)
Mediterranean	-100	0	Amensalism (B.a)
Western	-84.002982	107.03677	Parasitism (F.p)
Gluten_free	658.404815	-61.858933	Parasitism (B.a)
High_Fat_Low_Carb	344.09992	-34.829316	Parasitism (B.a)
High_Fiber	1231.90549	-56.387385	Parasitism (B.a)
T2D	331.25241	-22.47215	Parasitism (B.a)
Vegan	79.0886282	-11.871162	Parasitism (B.a)
Vegetarian	645.466855	-95.037258	Parasitism (B.a)
High_fiber_Agora	-89.686551	106.797944	Parasitism (F.p)
Western_Agora	-54.379504	62.5669725	Parasitism (F.p)

*F.prausnitzii* did not grow at all — amensalism and the Western and Agora’s high fibre diets where *F.prausnitzii* was the parasite). Although *B.adolescentis* behaves like a parasite in the co-culture, *F. prausnitzii* dominates the co-cultures in most diets. *Bifidobacteria* have been reported (Rivière et al. (2016)) to engage in competitive interactions with butyrate producers, so this outcome comes as a surprise.

### 3.3 Testing The Black Queen Hypothesis

Deleting genes responsible for intrinsic acetate production in *F.prausnitzii* resulted in no growth of either organism in co-culture for most of the diets. The only tolerated gene deletion was of ACKr, whose mutants could grow with *B. adolescentis* in the four dietary conditions as depicted in fig. 6. The figure compares species composition in the WT community and the community in which ACKr is knocked off in *F.prausnitzii*. It is seen that in these four conditions, there is no significant drop in the maximal butyrate production. However, the relative abundance of *F.prausnitzii* drops in the community after the KO. This, together with the fact that either organism fails to grow in the remaining diets suggests:

- ACKr might play some other essential role in *F. prausnitzii*, which is of use in most other diets. The pathways which are essential for an organism to thrive largely depends on the nutritional source. So, it could be that ACKr and the other acetate-producing genes may catalyse some reactions that are crucial in those diets but are compensated by the nutrients in the diets in fig. 6.

- Deletion of ACKr or other acetate-producing genes, in some diets, cause the extinction of *B. adolescentis*. This strange observation is suggestive that the deletions make *F. prausnitzii* consume all acetate from the medium, leaving nothing for *B. adolescentis* and may further consume all the acetate which the latter produces.

In sum, there is potential scope for the BQH when one of the four diets in fig. 6 is adopted.

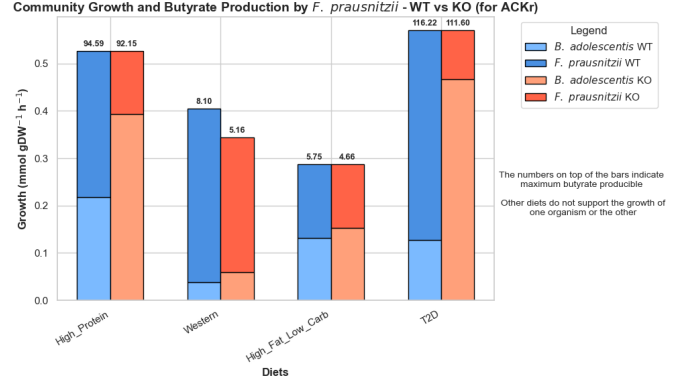


Fig. 6. Community Growth and Butyrate Production by *F. prausnitzii* - WT vs KO (for ACKr)

### 3.4 Investigating the flux distributions in the gluten-free and high-fibre diets

The gluten-free and high-fibre diets supported butyrate production the most. The former assisted in slightly higher butyrate flux compared to the latter. So, the flux distributions of the butyrate and acetate production pathways in both species were compared in the two nutritional conditions — fig. 7 and fig. 8. This was done to shed light upon what goes on metabolically in both organisms in the two diets. The key findings are:

- When *F. prausnitzii* grows in the gluten-free diet, there is zero flux in the reaction catalysing PEP to pyruvate. Instead, all flux from PEP is rerouted to OAA. From OAA, the flux is distributed between the aspartate pathway and towards pyruvate. On the other hand, in the high-fibre diet, this conversion from OAA to Pyr does not occur at all, and some of PEP gets converted to OAA, and others to pyruvate.
- The production of butyrate by *F. prausnitzii* requires acetate and Bt-CoA as precursors. Upon tracking back the reactions, it was noted that the slightly increased glycolysis in the gluten-free diet resulted in a greater supply of these two metabolites and in turn, butyrate. This stems directly from the fact that the gluten-free diet is possibly richer in polysaccharides, which break down into glucose or fructose and enter glycolysis.
- Fig. 5 suggests that in the gluten-free diet, *B. adolescentis* secretes more acetate than in the high-fibre diet. So the internal acetate-producing pathways in *B. adolescentis* were tracked. Yet again, the increased production of acetate in the gluten-free diet could be traced back to glycolysis. The higher the C-source, the higher the acetate production.

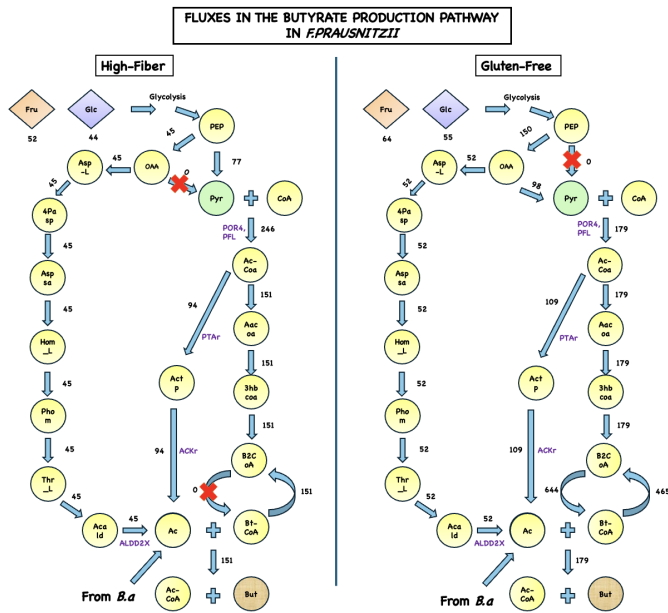


Fig. 7. Fluxes in the butyrate production pathway in *F. prausnitzii*

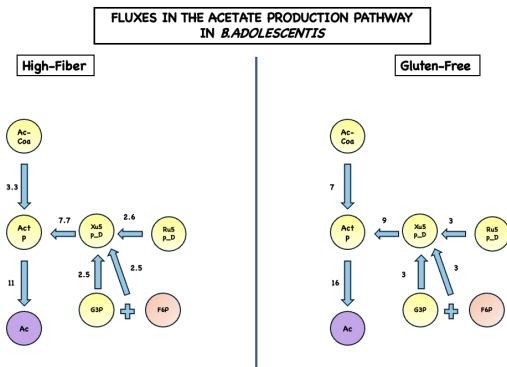


Fig. 8. Fluxes in the acetate production pathway in *B. adolescentis*

### 3.5 Dynamic FBA simulations — Monocultures

Next, true to the title of the project, the author wished to get a dynamic picture of the organisms, mainly in terms of growth and butyrate production. FBA tells us what is happening at one steady state. However, COMETS performs step-wise FBA, enabling us to simulate the gut's chemostat-like environment by incorporating parameters such as dilution rate and duration of the simulation. The two organisms were grown in monoculture starting at three initial concentrations — 0.01, 0.02 and 0.1 gDW as shown in the first two panels of fig. 9. Growth was carried out for 50 hours (500 cycles \* 0.1 timestep). Since the gluten-free diet did not work well on COMETS, the high-fibre diet was utilised in all dynamic simulations. It can be seen that both organisms' biomass steadily dwindles with time (this was noticed for a few other diets as well) at the same rate. This is quite natural as gut bacteria always exist in multi-membered communities where significant cross-feeding takes place to sustain each other.

Growth Curves of Monocultures at Different Initial Biomasses

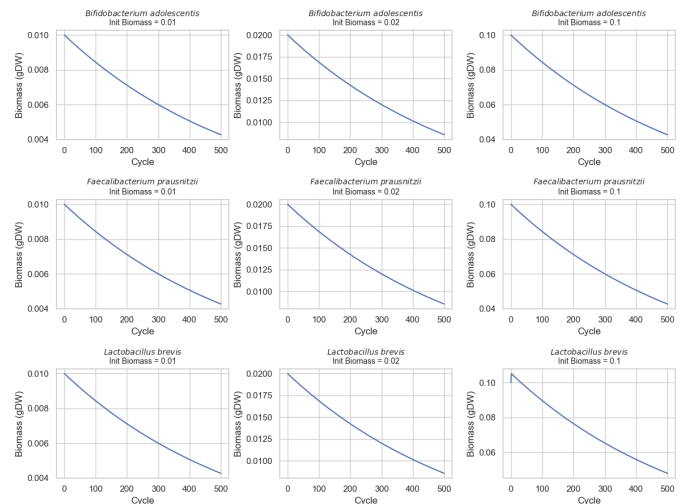


Fig. 9. Growth of the three organisms in monoculture at different initial biomasses

When monitoring the butyrate fluxes of *F. prausnitzii* across all initial biomass concentrations, we can see from fig. 10 that the flux values remain steadily at around  $78 \text{ mmol} \cdot \text{gDW}^{-1} \cdot \text{h}^{-1}$ , occasionally dropping to zero at some timepoints. When starting with 0.1 gdw, the flux oscillates and eventually drops to almost zero in cycle 90 ( $t=9\text{h}$ ) after which it increases but with oscillations. The monoculture flux predicted by normal FBA from fig. 3 for this diet is just slightly above  $50 \text{ mmol} \cdot \text{gDW}^{-1} \cdot \text{h}^{-1}$ . Yet, we cannot be satisfied since *F. prausnitzii*'s growth keeps declining with time.

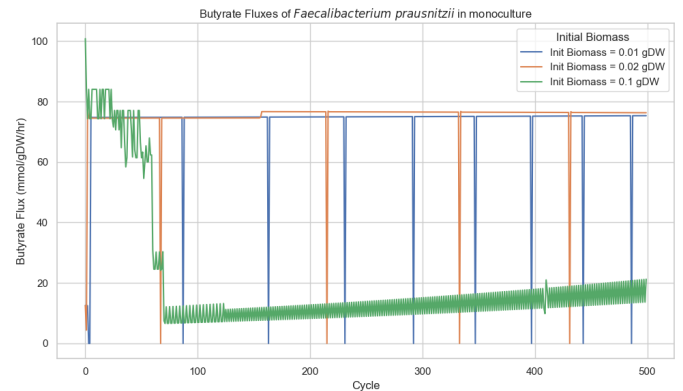


Fig. 10. Monoculture Butyrate flux by *F. prausnitzii*

### 3.6 Dynamic FBA simulations — Co-culture

#### Starting with the same initial biomass for both species

Next up, a community layout was created comprising both species in equal proportions, here, 0.02 gdw. The simulation was carried out for 1000 cycles or 100 h. The biomass trend of both species, as evident from fig. 11, both decline at the same rate. This is not suitable.

When the butyrate and acetate exchange fluxes were plotted in fig/ 12, butyrate secretion increases till 1.8h, after

which it drops down to almost zero, increases very slowly, but does not reach the initial levels. After cycle 800 (80h), it drops to zero.

Till 1.8h, when butyrate fluxes increase, *F. prausnitzii* uptakes acetate (flux value is negative) from *B. adolescentis*. After this, *F. prausnitzii* starts secreting more acetate than *B. adolescentis*. This suggests that instead of converting to butyrate, *F. prausnitzii* begins secreting all acetate. This scenario is clearly not desirable.

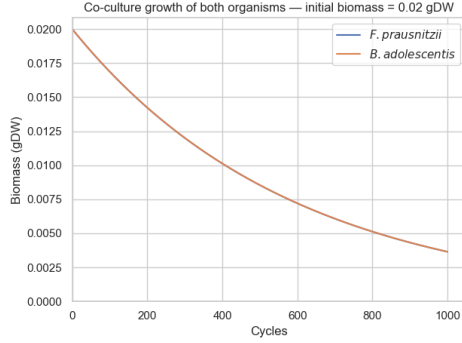


Fig. 11. Co-culture growth of both organisms at different initial biomasses

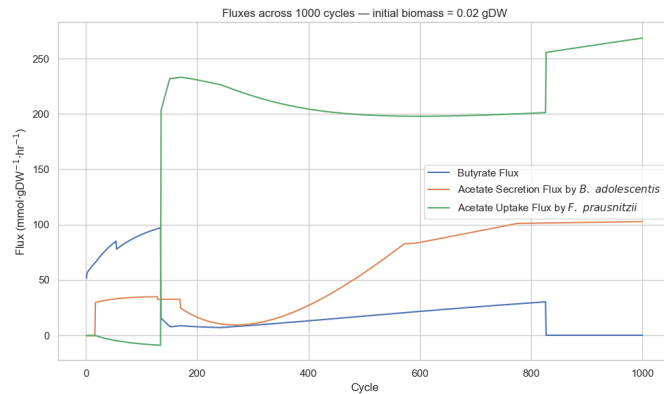


Fig. 12. Butyrate and acetate exchange fluxes when both species start with same initial biomass

### Starting with different initial biomass for both species

The subsequent step was to experiment as to what happens when *B. adolescentis* is present much higher (0.1 gDW) than *F. prausnitzii* (0.02 gDW). The logic behind this being, more the *B. adolescentis*, more support *F. prausnitzii* can derive to produce butyrate. Fig. 13 shows the biomass trend of both species.

Fig. 14 illustrates the butyrate and acetate fluxes of both species. We can notice a beautiful trend with butyrate fluxes steadily increasing to as high as 175 mmol-gDW<sup>-1</sup>·h<sup>-1</sup>. This is much higher than monoculture butyrate production. There is also a neat correlation between acetate release by *B. adolescentis* and uptake by *F. prausnitzii*. Butyrate release drops to almost zero around t=90h. This is the same timepoint when the biomass of *F. prausnitzii* drops very low. This situation is definitely better than the previous co-culture simulation in terms of

butyrate production but yet the biomass trends are not desirable as they decrease with time and do not grow.

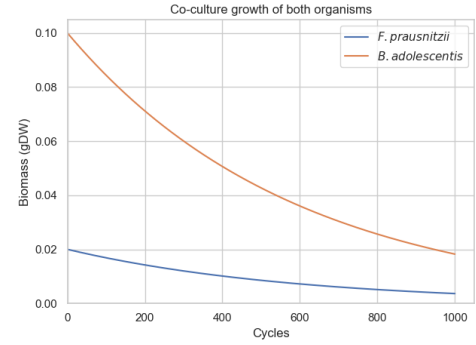


Fig. 13. Co-culture growth of both organisms at different initial biomasses

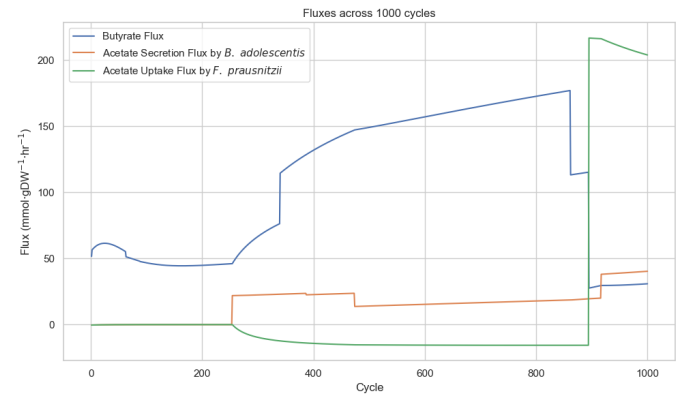


Fig. 14. Butyrate and acetate exchange fluxes at different initial biomasses

### 3.7 Dynamic FBA simulations — introducing *Lactobacillus brevis*

#### Starting with a three-membered community

*Lactobacillus brevis* is a probiotic and is found in curd as well. The primary reason behind choosing this species for invasion is because it produces D-lactate, which can be consumed by *F. prausnitzii* for butyrate production. *B. adolescentis* secretes only L-lactate, which cannot be consumed by *F. prausnitzii*. There were two really fascinating observations:

- When a community of all three species was simulated, an increase in biomass was finally observed! The first two species began growing as well! This proves that complex community interactions, such as cross-feeding, which dominate the gut, are vital for the survival of the organisms.
- In COMETS, after creating a community layout, the species are added one by one to it. In an intriguing turn of events, it was seen that the order of species addition decided the trend in growth of the entire community. Two such cases are shown in fig. 15 and fig. 16. Further investigation suggested that it could be an outcome of the first species getting added gaining more advantage to the medium than the others and this could impact the overall community dynamics.



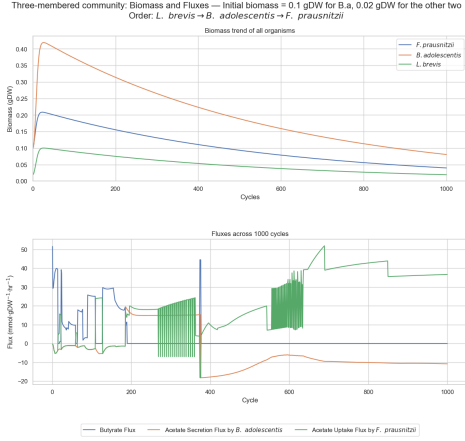


Fig. 15. One order of addition: biomass and key fluxes

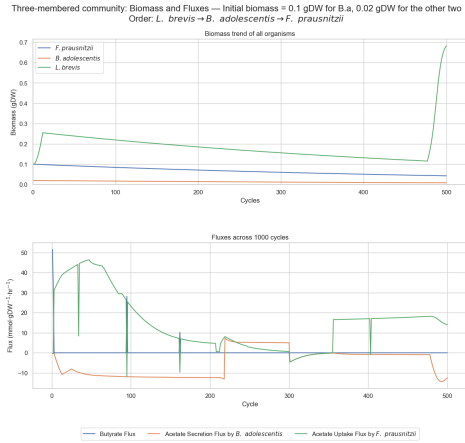


Fig. 16. Another order of addition: biomass and key fluxes

## Sequential Invasion

Since the order of addition at the very beginning ( $t=0h$ ) itself resulted in strikingly different growth trends, the author wanted to add one species and allow it to grow for some time before adding the next and observe the consequences. This kind of sequential invasion was carried out in all possible combinations ( $\binom{3}{2} = 6$ ). Each species was allowed to grow for 200 cycles (20h) before the next species was added. Hence, the total simulation duration was 600 cycles (60h). The initial biomass concentrations of all species were set to 0.02 gDW. (The number of cycles could not be increased beyond this as COMETS began to crash, unfortunately, for very high simulation durations.) Fig. 17 and 18 show the biomass trends of the three species and the butyrate fluxes in all six possible sequences of invasion. Now, we need to pick the sequence order in which all three species grow and which supports a reasonable production of butyrate.

It can be seen that sequences: 1-2-0, followed by 2-1-0 and 1-0-2, support decent growth of all three species (0: *B. adolescentis*, 1: *F. prausnitzii*, 2: *L. brevis*). These three sequences support high butyrate production in the order 1-2-0 1-0-2 2-1-0. We can conclude 1-2-0 is the best possible sequence of invasion that serves the purpose of species growth as well as butyrate production.

Biomass Trend Across Invasion Sequences  
0: *B. adolescentis*, 1: *F. prausnitzii*, 2: *L. brevis*

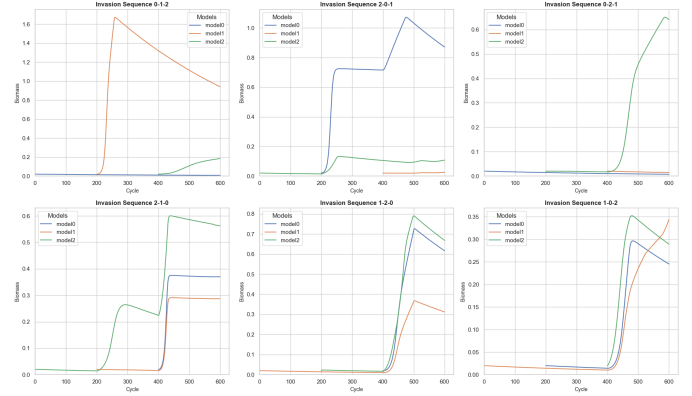


Fig. 17. Biomass Trend Across Invasion Sequences (Initial biomass conc. for all = 0.02 gDW)

Butyrate Flux Across Invasion Sequences  
0: *B. adolescentis*, 1: *F. prausnitzii*, 2: *L. brevis*

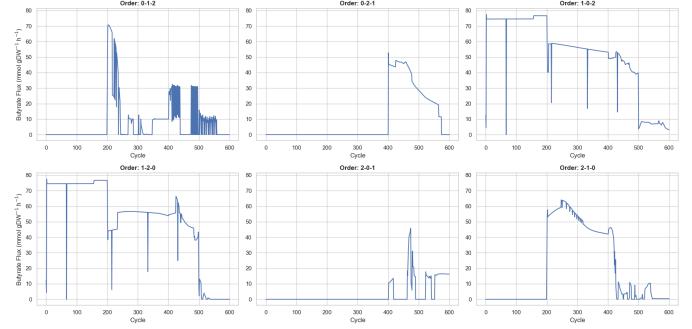


Fig. 18. Butyrate Fluxes Across Invasion Sequences (Initial biomass conc. for all = 0.02 gDW)

## Key takeaways:

- The general pattern is that whenever *F. prausnitzii* is the pioneer species or when *L. brevis* is the pioneer and *F. prausnitzii* is its immediate successor, all three organisms thrive and butyrate production is optimum.
- When we closely examine the butyrate flux values, they are comparable to the values of *F. prausnitzii* in monoculture and less than what was noted in the best-case scenario in the two-membered community (of *F. prausnitzii* and *B. adolescentis*). However, we must remind ourselves that the species never grew in all those previous conditions. In the three-membered set-up, in some combinations, they exhibit excellent growth and certain consistency in butyrate production. Hence, a clear trade-off is demonstrated.

## 4. CONCLUSION AND FURTHER SCOPE

This quest began with several questions posed as objectives. The main outcome of the work is that optimal butyrate production and species growth are observed when *F. prausnitzii* is the pioneer species, or when it is the first invader of a *L. brevis* filled environment. We identified a trade-off between growth and butyrate production, and the most compatible diet being the high-fibre diet. Hence,

we get insights as to how to time the intake of the different bacteria and which diet suits the purpose best. There is still a lot of scope in the dynamic simulations. For instance, the initial proportions of the three species can be further refined to ensure even more sustained butyrate production. Further, other bacterial species can be considered as invaders, and the same studies can be carried out. The ultimate aim is to design a suitable cohort of bacteria which can be administered as probiotics to address neurological disorders. Towards this lofty goal, the author hopes that this work would be of use, at least in a minor way.

## ACKNOWLEDGEMENTS

I express my sincere gratitude to Dr. Karthik Raman for his constant motivation and for providing a strong foundation in all the concepts needed to carry out this work. I am also deeply thankful to Dr. Maziya Ibrahim and Ms. Sabdhayini K B for their very valuable insights and guidance.

## REFERENCES

- Dukovski, I., Bajić, D., Chacón, J.M., Quintin, M., Vila, J.C., Sulheim, S., Pacheco, A.R., Bernstein, D.B., Riehl, W.J., Korolev, K.S., Sanchez, A., Harcombe, W.R., and Segrè, D. (2021). A metabolic modeling platform for the computation of microbial ecosystems in time and space (comets). *Nature Protocols* 2021 16:11, 16, 5030–5082. doi:10.1038/s41596-021-00593-3. URL <https://www.nature.com/articles/s41596-021-00593-3>.
- Duranti, S., Ruiz, L., Lugli, G.A., Tames, H., Milani, C., Mancabelli, L., Mancino, W., Longhi, G., Carnevali, L., Sgoifo, A., Margolles, A., Ventura, M., Ruas-Madiedo, P., and Turróni, F. (2020). Bifidobacterium adolescentis as a key member of the human gut microbiota in the production of gaba. *Scientific Reports*, 10, 1–13. doi:10.1038/S41598-020-70986-Z; SUBJMETA=325,326,631;KWRD=MICROBIAL+GENETICS,MICROBIOLOGY. URL <https://www.nature.com/articles/s41598-020-70986-z>.
- Hazan, S., Stollman, N., Bozkurt, H.S., Dave, S., Papoutsis, A.J., Daniels, J., Barrows, B.D., Quigley, E.M., and Borody, T.J. (2022). Lost microbes of covid-19: Bifidobacterium, faecalibacterium depletion and decreased microbiome diversity associated with sars-cov-2 infection severity. *BMJ Open Gastroenterology*, 9. doi:10.1136/BMJGAST-2022-000871. URL <https://pubmed.ncbi.nlm.nih.gov/35483736/>.
- He, X., Zhao, S., and Li, Y. (2021). Faecalibacterium prausnitzii: A next-generation probiotic in gut disease improvement. *Canadian Journal of Infectious Diseases and Medical Microbiology*, 2021, 6666114. doi:10.1155/2021/6666114. URL <https://onlinelibrary.wiley.com/doi/abs/10.1155/2021/6666114https://onlinelibrary.wiley.com/doi/10.1155/2021/6666114>.
- Heirendt, L., Arreckx, S., Pfau, T., Mendoza, S.N., Richelle, A., Heinken, A., Haraldsdóttir, H.S., Wachowiak, J., Keating, S.M., Vlasov, V., Magnúsdóttir, S., Ng, C.Y., Preciat, G., Zagare, A., Chan, S.H., Aurich, M.K., Clancy, C.M., Modamio, J., Sauls, J.T., Noronha, A., Bordbar, A., Cousins, B., Assal, D.C.E., Valcarcel, L.V., Apaolaza, I., Ghaderi, S., Ahookhosh, M., Guebila, M.B., Kostromins, A., Sompairac, N., Le, H.M., Ma, D., Sun, Y., Wang, L., Yurkovich, J.T., Oliveira, M.A., Vuong, P.T., Assal, L.P.E., Kuperstein, I., Zinovyev, A., Hinton, H.S., Bryant, W.A., Artacho, F.J.A., Planes, F.J., Stalidzans, E., Maass, A., Vempala, S., Hucka, M., Saunders, M.A., Maranas, C.D., Lewis, N.E., Sauter, T., Palsson, B., Thiele, I., and Fleming, R.M. (2019). Creation and analysis of biochemical constraint-based models using the cobra toolbox v.3.0. *Nature Protocols* 2019 14:3, 14, 639–702. doi:10.1038/s41596-018-0098-2. URL <https://www.nature.com/articles/s41596-018-0098-2>.
- Magnúsdóttir, S., Heinken, A., Kutt, L., Ravcheev, D.A., Bauer, E., Noronha, A., Greenhalgh, K., Jäger, C., Baginska, J., Wilmes, P., Fleming, R.M., and Thiele, I. (2017). Generation of genome-scale metabolic reconstructions for 773 members of the human gut microbiota. *Nature Biotechnology*, 35, 81–89. doi:10.1038/NBT.3703;TECHMETA=58,82; SUBJMETA=2565,2695,2710,326,553,631;KWRD=BIOCHEMICAL+NETWORKS,MICROBIAL+COMMUNITIES,COMPUTER+MODELLING. URL <https://www.nature.com/articles/nbt.3703>.
- Rios-Covian, D., Gueimonde, M., Duncan, S.H., Flint, H.J., and Reyes-Gavilan, C.G.D.L. (2015). Enhanced butyrate formation by cross-feeding between faecalibacterium prausnitzii and bifidobacterium adolescentis. *FEMS Microbiology Letters*, 362. doi:10.1093/FEMSLE/FNV176. URL <https://pubmed.ncbi.nlm.nih.gov/26420851/>.
- Rivière, A., Selak, M., Lantin, D., Leroy, F., and Vuyst, L.D. (2016). Bifidobacteria and butyrate-producing colon bacteria: Importance and strategies for their stimulation in the human gut. *Frontiers in Microbiology*, 7, 979. doi:10.3389/FMICB.2016.00979. URL <https://pmc.ncbi.nlm.nih.gov/articles/PMC4923077/>.
- Sambamoorthy, G. and Raman, K. (2022). Deciphering the evolution of microbial interactions: in silico studies of two-member microbial communities. *bioRxiv*, 2022.01.14.476316. doi:10.1101/2022.01.14.476316. URL <https://www.biorxiv.org/content/10.1101/2022.01.14.476316v1https://www.biorxiv.org/content/10.1101/2022.01.14.476316v1.abstract>.
- Shao, Y., Garcia-Mauriño, C., Clare, S., Dawson, N.J., Mu, A., Adoum, A., Harcourt, K., Liu, J., Browne, H.P., Stares, M.D., Rodger, A., Brocklehurst, P., Field, N., and Lawley, T.D. (2024). Primary succession of bifidobacteria drives pathogen resistance in neonatal microbiota assembly. *Nature Microbiology* 2024 9:10, 9, 2570–2582. doi:10.1038/s41564-024-01804-9. URL <https://www.nature.com/articles/s41564-024-01804-9>.
- Singh, R., Dutta, A., Bose, T., and Mande, S.S. (2022). A compendium of predicted growths and derived symbiotic relationships between 803 gut microbes in 13 different diets. *Current Research in Microbial Sciences*, 3, 100127. doi:10.1016/J.CRMICR.2022.100127. URL <https://www.sciencedirect.com/science/article/pii/S2666517422000244>.
- Singh, V., Lee, G.D., Son, H.W., Koh, H., Kim, E.S., Unno, T., and Shin, J.H. (2023). Butyrate producers, “the sentinel of gut”: Their intestinal significance with and beyond butyrate, and prospective use as microbial therapeutics. *Frontiers in Microbiology*, 13, 1103836. doi:10.3389/FMICB.2022.1103836. URL <https://pmc.ncbi.nlm.nih.gov/articles/PMC9877435/>.